Biochimica et Biophysica Acta, 1063 (1991) 36–44

ADONIS 000527369100131H

BBAMEM 75171

Ion channel formation by synthetic transmembrane segments of the inhibitory glycine receptor – a model study

Dieter Langosch [1], Klaus Hartung [2], Ernst Grell [2], Ernst Bamberg [2] and Heinrich Betz [1]

[1] *ZMBH, Universität Heidelberg, Heidelberg (F.R.G.) and* [2] *Max-Planck-Institut für Biophysik, Frankfurt (F.R.G.)*

(Received 17 August 1990)
(Revised manuscript received 14 November 1990)

Key words: Channel protein; Ion channel; Glycine receptor; (Rat)

The inhibitory glycine receptor (GlyR) of rat spinal cord contains an intrinsic transmembrane channel mediating agonist-gated anion flux. Here, synthetic peptides modelled after the predicted transmembrane domains M2 and M4 of its ligand-binding subunit were incorporated into lipid vesicle membranes and black lipid bilayers to analyze their channel forming capabilities. Both types of peptides prohibited the establishment of, or dissipated, preexisting transmembrane potentials in the vesicle system. Incorporation of peptide M2 into the black lipid bilayer elicited randomly gated single channel events with various conductance states and life-times. Peptide M4 increased the conductance of the bilayer without producing single channels. Exchange of the terminal arginine residues of peptide M2 by glutamate resulted in a significant shift towards cation selectivity of the respective channels as compared to peptide M2. In conclusion, the peptide channels observed differed significantly from native GlyR in both conductivity and ion-selectivity indicating that individual synthetic transmembrane segments are not sufficient to mimic a channel protein composed of subunits with multiple transmembrane segments.

Introduction

Ion channel proteins regulate passive ion transport across biological membranes. It is generally assumed that an assembly of hydrophobic peptide segments long enough to span the core of a lipid bilayer in an ordered secondary structure anchors the channel protein in the membrane and provides the lining of its intrinsic pore. For example, six putative α-helical transmembrane segments characterize the repeat domains or subunits of voltage-gated ion channels in excitable membranes [1]. Four such segments (M1–M4) are found within the subunits of different ligand-gated ion channel proteins – the nicotinic acetylcholine receptor (nAChR; Refs. 2–4), the glycine receptor (GlyR; Ref. 5), and the γ-aminobutyric acid receptor ($GABA_AR$; Ref. 6). In the nAChR, segment M2 has been proposed to form the channel wall based on covalent labelling experiments with channel blockers [7,8] and ion-permeation studies on chimeric receptors [9]. Within the inhibitory ligand-gated anion channel proteins, the GlyR and the $GABA_AR$, this segment displays an accumulation of hydroxylated amino acids suited to provide a hydrophilic channel wall as well as strong sequence conservation between subunits. Therefore, segment M2 is thought to line the wall of GlyR and $GABA_AR$ channels also [5,6]. The hydrophobic segment M4, in contrast, is assumed to be localized at the protein/lipid interface of the receptor's transmembrane portion.

The GlyR consists of two types of glycosylated membrane-spanning subunits of M_r 48000 (α) and 58000 (β) which are arranged in a pentameric transmembrane structure [10,11]. Photoaffinity labelling experiments with [^{3}H]strychnine [12] and heterologous expression in *Xenopus* oocytes [13] and mammalian cells [14] define the M_r 48000 polypeptide as a ligand-binding subunit capable of forming a functional GlyR. The single-channel properties of the GlyR have been investigated in detail by patch clamp analysis of embryonic mouse spinal cord cultures [15]. Specifically, the channel was

Abbreviations: CD, circular dichroism; $GABA_AR$, γ-aminobutyric acid receptor; GlyR, glycine receptor; diS-C_3(5), 3,3'-dipropylthiadicarbocyanine iodide; EGTA, ethyleneglycol bis(β-aminoethyl ether)tetraacetic acid; Hepes, 4-(2-hydroxyethyl)-1-piperazineethanesulfonic acid; Mes, 4-morpholineethanesulfonic acid; nAChR, nicotinic acetylcholine receptor.

Correspondence: D. Langosch, Max-Planck-Institut für Hirnforschung, Abt. Neurochemie, Heinrich-Hoffmann-Str. 46, D-6000 Frankfurt 71, F.R.G.

found to be selective for monovalent anions, and various subconductance states with a main single-channel conductance of 45 pS in 145 mM chloride solution were observed [16]. The existence of at least two sequentially occupied anion binding sites in the channel has been postulated [15] and proposed to be the functional correlate of positively charged amino acids bordering the M2 segment of the α subunit intra- and extracellularly [5].

Recently, attempts have been made to reconstitute the channel function of the voltage-gated Na^+ channel and of the nAChR by incorporation of peptides corresponding to the putative pore lining segments of these proteins into lipid bilayers [17,18]. In both cases the observed channel activities were suggested to mimick functional properties of the native proteins.

In this study, we describe the conformational and channel forming properties of synthetic peptides corresponding to the sequences of the putative transmembrane segments M2 and M4 of the GlyR α subunit. All peptides tested were found to increase the ion conductivity of lipid bilayers. Interestingly, the ion selectivity of the M2 peptide channels was modulated by the terminal charges of the transmembrane sequence.

Methods

Peptide synthesis

Peptides were synthesized from 9-fluoromethoxycarbonyl amino acids (NovaBiochem, Switzerland) by solid phase methods [19] on an automated peptide synthesizer (Applied Biosystems, model 430A). Cleavage from the resin and deprotection was achieved with anhydrous trifluoroacetic acid. The peptides were purified by high-pressure liquid chromatography using a Nucleosil C_{18} reverse phase column (250×20 mm; Latek, Heidelberg, F.R.G.) for peptides M2 and M2-Glu, and a C_4 column for peptide M4, respectively. Peptides were eluted using linear gradients of acetonitrile in 1% (v/v) trifluoroacetic acid, and their identity confirmed by amino acid analysis.

CD measurements

Peptide stock solutions of about 0.4 mM peptide were prepared in trifluoroethanol (Uvasol quality, Merck) and diluted 10-fold before the measurement either by addition of the same solvent or of 5 mM sodium phosphate buffer (pH 7.4). Spectroscopy was carried out in a 2 mm cuvette at 25°C employing a Jasco J 500 A spectropolarimeter. CD intensities [θ] are expressed as mean residue ellipticity (degree $cm^2\ dm^{-1}$) by calculating the molar ellipticity according to Adler et al. [20].

Permeability studies on lipid vesicles

(a) Peptide incorporation by dialysis. Aliquots of 2.5 mg egg phsphatidylcholine (Sigma) dissolved in $CHCl_3$ were dried under a stream of nitrogen and evacuated for 1 h to remove traces of the solvent. Peptides were dissolved by sonication in a solution of 10 mM Mes-NaOH (pH 6.0), 250 mM KCl, 1 mM $MgCl_2$, 0.1 mM EGTA, 5% (w/v) 3-(3-cholamidopropyl)dimethylammonio-1-propane sulfonate (Serva), and 6% (w/v) octyl glucoside (Sigma) to various concentrations, and the solutions filtered through 0.45 μm Millipore filters. Aliquots of 0.5 ml of these peptide solutions or a control solution, respectively, were added to the dried lipids, the mixtures were shaken for 30 min in an Eppendorf mixer, and bath-sonified for 10 min. The clear solutions were then dialyzed (Spektra-Por dialysis tubing, 2 kDa cutoff weight) against 3×3 l Mes-NaOH (pH 6.0), 250 mM KCl, 1 mM $MgCl_2$, 0.1 mM EGTA, at 4°C for 90 h, and the resulting vesicle suspensions subjected to ten successive freeze-thaw cycles in liquid nitrogen.

(b) Preparation of vesicles by sonication. A solution of 100 mM KCl was added to egg phosphatidylcholine (Serva) spread onto the walls of a tube as described above to yield a lipid concentration of 5 mg/ml. After incubation at 37°C for hydration and brief vortexing, the lipid suspension was sonicated under cooling for approx. 10 min using the cup horn attachment of a Bransonic B15 cell disruptor (power setting 10). Finally, the vesicle suspension was subjected to one freeze-thaw cycle in liquid nitrogen.

(c) Measurement of membrane potential. Fluorescence measurements were carried out with a Shimadzu RF-5000 spectrofluorometer with permanently stirred glass cuvettes using excitation and emission wavelengths of 622 nm and 660 nm, respectively. To 1 ml of 10 mM Mes-NaOH (pH 6.0), 1 mM $MgCl_2$, 0.1 mM EGTA, balanced to isoosmolarity with mannitol and containing 0.5 μM of the fluorescent dye 3,3'-dipropylthiadicarbocyanine iodide (diS-C_3(5), Molecular Probes, Eugene, OR) were added 2 μl of the respective vesicle suspensions and, after 80 s, 10^{-11} M gramicidin (EGA, Switzerland) dissolved in ethanol. The development of inside-negative potentials was monitored by measuring the decrease in fluorescence intensity of the dye [21]. Peptides were added dissolved at 20 μM in ethanol (M2) or ethanol/DMSO 3:1 (M4).

Bilayer experiments

Bilayers of the Mueller-Rudin type [22] were formed across an aperture separating two half-cells of a teflon cuvette. The hole was pretreated with 0.5% (w/v) dioleoylphosphatidylethanolamine in hexane, and membranes were made from a 2% (w/v) solution of dioleoylphosphatidylethanolamine and dioleoylphosphatidylcholine (Avanti Polar Lipids, Birmingham, AL) at a ratio of 3:1 in *n*-decane. The bilayers used had a conductivity of approx. 10 pS and a capacity of approx. 0.5 $\mu F/cm^2$. Both half-cells were filled with 5 ml each

of 10 mM Mes-NaOH (pH 6.0), 100 mM KCl. The cuvette was connected to the measuring circuit with Ag/AgCl-electrodes via salt bridges. The cis-side of the cuvette was connected to a variable voltage source, and the trans-side to a current-to-voltage converter with a 1 GΩ feedback resistor. All measurements were performed at room temperature.

Peptides were incorporated into lipid vesicles and the latter fused to the bilayer as follows. To dried egg phosphatidylcholine (Serva) solutions of 250 mM or 500 mM KCl in 20 mM Hepes-NaOH (pH 8.0), were added to yield final concentrations of 10 mg/ml of lipid. After hydration, sonication, and freeze-thawing as described above, the vesicles were bath-sonified for 15 s. Subsequently, the vesicles were diluted 10-fold in 250 and 500 mM KCl, respectively, in 20 mM Hepes-NaOH (pH 8.0), and individual peptides (dissolved in ethanol, or ethanol/dimethyl sulfoxide 3:1) were added to final concentrations from 1–5 μM. Aliquots (5–10 μl) of the vesicle suspensions were introduced into the electrolyte solution of the cis compartment of the bilayer cuvette and the solutions stirred for 5 min. To initiate fusion, the cis compartment was made 200 mM in urea and stirring continued for 30 min [23]. In case no increased conductivity was seen at this point, another 5–10 μl of the vesicle suspensions were added and stirring continued for another 30 min. Fluctuating or stably increased conductivities were routinely observed after this procedure. To stop further fusion, the trans side was made isoosmotic to the cis side by addition of urea.

To determine reversal potentials, the offset currents generated by a KCl gradient across the lipid bilayer were compensated to zero by external voltages applied to that side of the bilayer containing the higher concentration of KCl (cis). The values thereby obtained were taken as reversal potentials after correction for electrode offset voltage measured after destroying the bilayer. Alternatively, current/voltage relationships were recorded in the presence of KCl gradients.

Results

Peptides corresponding to the putative transmembrane sequences M2 (ARVGLGITTVLTMTTQSSGSRA) and M4 (RIGFPMAFLIFNMFYWIIYK) of the GlyR α subunit [5] were synthesized by automated solid phase chemistry. To investigate the potential function of charged amino acid head groups, a derivative of peptide M2 was also synthesized, in which both terminal arginine residues were replaced by glutamate (M2-Glu). All peptides were subjected to structural and functional analysis as follows.

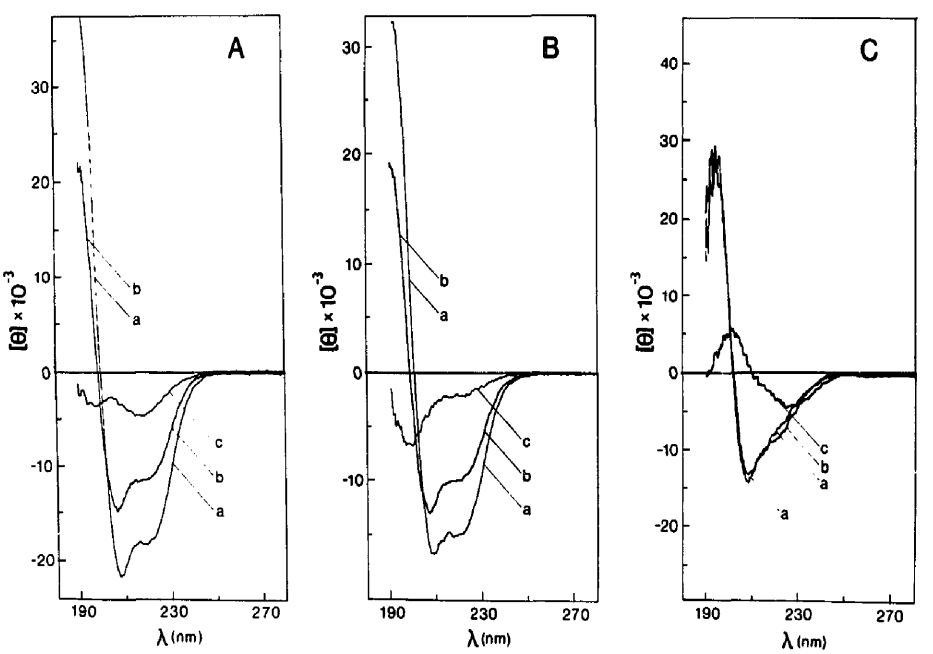

Fig. 1. CD spectra recorded at 25°C of M2 (A), M2-Glu (B) and M4 (C) in trifluoroethanol (a); 50% (v/v) 5 mM phosphate buffer (pH 7.4) in trifluoroethanol (b); and 90% (v/v) 5 mM phosphate buffer (pH 7.4) in trifluoroethanol (c). [θ] represents the mean residue ellipticity.

CD measurements

CD spectra reflect the conformational properties of peptides and proteins and were recorded here to evaluate the general secondary structure of the three peptides. Fig. 1 shows their CD spectra in various mixtures of trifluoroethanol with phosphate buffer. Based on reference spectra [20,24], secondary structure can be analyzed in terms of α-helix, β-chain, and random coil content. An interpretation of the CD spectra shown in Fig. 1A and B yielded for M2 and M2-Glu, in pure trifluoroethanol, α-helix contents of roughly 50% with random coil and some β-sheet conformations accounting for the majority of residual secondary structure. The CD spectrum of peptide M4 appeared atypical (Fig. 1C) but suggests an ordered structure. Its interpretation was complicated further by the presence of many aromatic side chains whose positive Cotton effect can severely distort the CD spectrum [20]. A greater apparent stability of M4 secondary structure can be deduced from the larger phosphate buffer content in the mixed solvent system required to rearrange its spectrum. Upon decreasing the trifluoroethanol concentration to 10% all spectra changed drastically with random coil structures prevailing (Fig. 1, trace c).

Ion flux across lipid vesicle membranes

Initially, we examined the basic capability of the peptides M2, M2-Glu, and M4 to increase the ion permeability of lipid vesicle membranes. The peptides were incorporated into egg phosphatidylcholine vesicles, and subsequently the ability of the doped vesicles to hold transmembrane potentials imposed by cation efflux was tested. First, the vesicles made in the presence of 250 mM KCl were diluted into an isoosmotic medium without KCl and the cation permeability of the vesicle membranes increased by adding the peptide ionophore gramicidin. In the case of control vesicles, formation of an inside negative potential was then detected by the decreasing fluorescence intensity of the potential-sensitive dye diS-C_3(5). No decrease in fluorescence intensity, indicating zero polarization of the membrane, was observed when peptides M2, M4, or M2-Glu had been

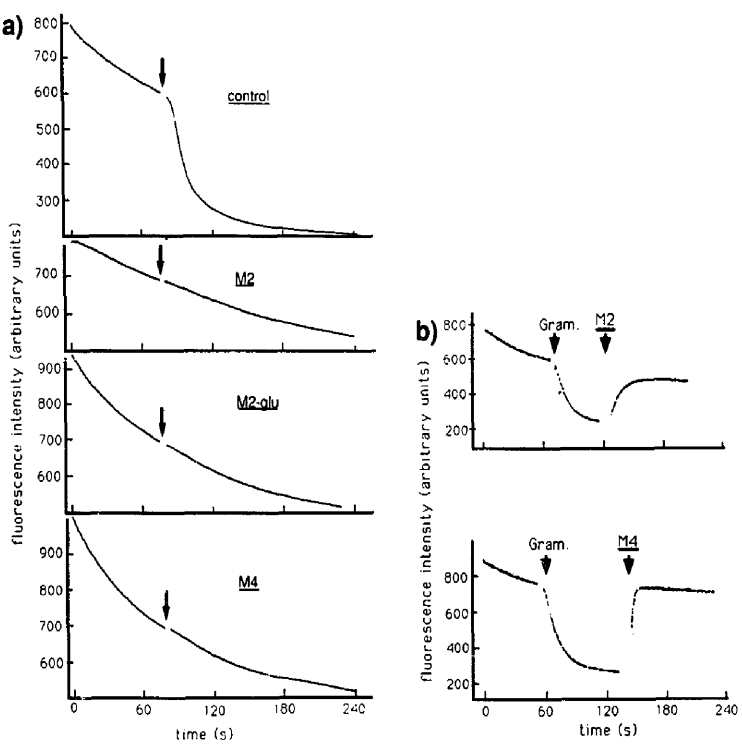

Fig. 2. Measurements of transmembrane potentials in lipid vesicle suspensions using the potential-sensitive dye diS-C_3(5) as described in Methods. (a) Decreasing fluorescence after addition of 10^{-11} M gramicidin (arrows) indicates the development of an inside-negative potential with control vesicles, but not with vesicles doped with peptide. (b) Addition of 0.1 μM of the peptides M2 or M4 to vesicles previously polarized with 10^{-11} M gramicidin resets fluorescence intensities to near original values.

incorporated into the vesicle membranes (Fig. 2a). We interpret this finding in that the peptides M2, M4, or M2-Glu all increase chloride permeability, thus impeding the formation of a K^+ diffusion potential by gramicidin. From a mean diameter of approx. 30 nm as determined by electron microscopy and, based on the weighted amounts of lipids and peptides used, a maximal number of approx. 40 peptide molecules per lipid vesicle was calculated for the preparations used in these experiments. At 20-fold lowered peptide concentrations, the gramicidin mediated decrease in fluorescence intensity approached that of control vesicles. Thus, a number between 2 and 40 peptide molecules per vesicle was sufficient to permit anion flux.

In another experiment, transmembrane potentials were first established by adding gramicidin to pure lipid vesicles. Subsequent addition of peptides M2 or M4 (0.1 μM) restored the fluorescence intensities to near original values (Fig. 2b). This demonstrates the capability of the added peptides M2 and M4 to dissipate preexisting transmembrane potentials. Here, a peptide/lipid ratio about 5-fold higher than that in the above experiments was required; this suggests the efficiency of peptide incorporation into preformed vesicle membranes being lower than with the detergent dialysis procedure. M2-Glu was found to be ineffective in the latter experiment; this might reflect the inability of this negatively charged peptide to insert into a preformed vesicle membrane.

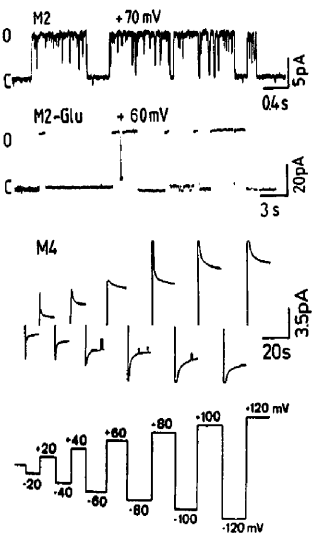

Fig. 3. Effects of peptides on bilayer conductance. Individual peptides were incorporated into planar bilayers by a vesicle fusion technique as described in Methods. M2: current fluctuations after incorporation of peptide M2 recorded at +70 mV. M2-Glu: current fluctuations elicited by peptide M2-Glu recorded at +60 mV. M4: stable bilayer conductance recorded after incorporation of peptide M4; transbilayer voltages are indicated below the trace. Current and time scales are indicated by bars for each experiment.

Channel formation in planar bilayers

Peptides M2, M2-Glu, and M4 were incorporated into black lipid membranes to investigate (i) single-channel behavior and (ii) ion-selectivities of the channels formed. To this end, the peptides were preincorporated in lipid vesicles and the latter fused to the bilayer. Using this protocol, incorporation of all peptides tested, but not fusion of control vesicles, was found to increase the conductivity of the bilayer.

The positively charged peptide M2 induced rectangular conductivity fluctuations indicative of single-channel activity (Fig. 3). These randomly gated events included variable conductances ranging from the lowest values detectable above background noise (approx. 12 pS) to above 1 nS; channel life-times between tens of milliseconds and seconds were observed. The fluctuations were not stationary as their amplitude distribution often changed within tens of seconds. This complexity prevented a detailed analysis of the gating behavior of these channels.

To assess the ion-selectivity of the peptide channels, concentration gradients of KCl were established across the bilayer and reversal potentials determined. From the latter, permeability ratios were calculated according to Goldman, Hodgkin and Katz [25]. The conductivity of bilayers containing several M2 channels could be changed by briefly increasing transbilayer voltage to approx. 100 mV. These conductivity changes were often accompanied by changes in permeability ratios; no steady correlation between both parameters was, however, detected. As shown in Fig. 4A, the conductances induced by the positively charged M2 peptide could be moderately anion-selective as well as cation-selective but were essentially non-selective ($P_K/P_{Cl} \approx 1.5$) in most measurements (5 bilayers, 30 determinations). One explanation for these divergent observations is that M2 peptides may form cation- as well as anion-selective channels and that the nonselectivity of most membranes is due to the simultaneous presence of both channel types. Alternatively, non-selectivity of the membrane may reflect nonselectivity of the respective single channels. To resolve this problem, we analyzed the ion selectivity of single channels. Fig. 4B shows channel-like conductance fluctuations which are recorded without applied voltage in the presence of a KCl gradient. This allows a qualitative determination of the ion selectivity from the direction of the current flow. Trace (a) shows cis to trans current fluctuations indicative of cation selectivity whereas trace (b) recorded from the same membrane 15 min later shows trans to cis currents indicating that an anion-selective channel had formed. In four different membranes, both channel types were also found to coexist in the same membrane (for exam-

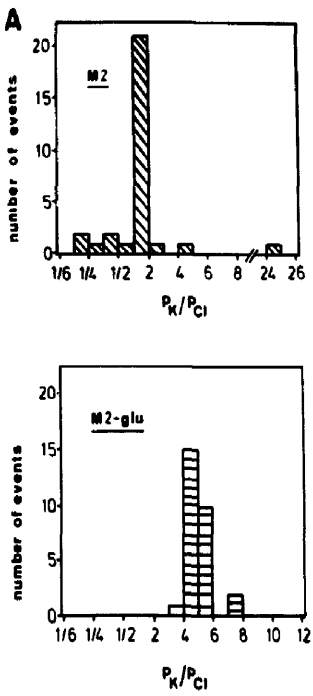

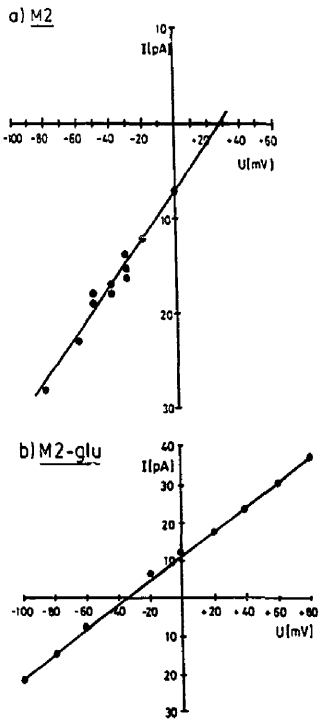

Fig. 5. Current/voltage relationships of single-channel events elicited by peptides M2 or M2-Glu in the presence of concentration gradients of KCl (M2, cis = 1.06 M KCl, trans = 0.17 M KCl; M2-Glu, cis = 0.88 M KCl, trans = 0.16 M KCl). For the experiments shown here, permeability ratios P_K/P_{Cl} of 0.2 and 12 were calculated for M2 channels and M2-Glu channels, respectively. The data shown are exemplary (see text).

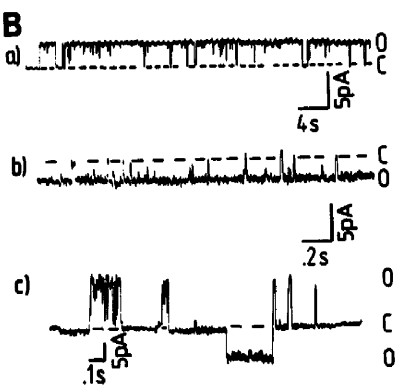

Fig. 4. Ion selectivity of peptide channels. (A) Histograms of permeability ratios P_K/P_{Cl} calculated from the reversal potentials determined for planar bilayers doped with the respective peptides after establishing KCl gradients in 10 mM Mes (pH 6.0) as described in the Methods and Results sections. 'Events' denotes the number of determinations corresponding to specific permeability ratios. (B) Induction of anion-selective and cation-selective conductances by M2. Current fluctuations were recorded in the presence of a KCl concentration gradient (0.1 M cis versus 0.6 M trans) without external voltage. Cation-selective fluctuations (trace a) are followed by anion-selective fluctuations (trace b) after 15 min in the same bilayer. Trace c is from the same experiment and shows both conductances in rapid succession. 'C' denotes the absolute zero current level.

ple: Fig. 4B, trace c). Fig. 5a displays one of two separately recorded current/voltage relations determined from membranes containing only one anion-selective M2 channel ($P_K/P_{Cl} \approx 0.2$). No complete current voltage relation could, however, be obtained for a cation-selective M2 channel due to the latter's kinetic instability. Apparently, peptide M2 is capable of forming different channel types prefering anions or cations, respectively. The simultaneous presence of both channel types in the bilayer may cause the variability of ion-selectivity seen in Fig. 4A.

In contrast to peptide M2, the negatively charged derivative M2-Glu induced very stable conductance fluctuations, the amplitude distribution being stable for many minutes. Often, one type of conductivity dominated (Figs. 3 and 6) and thus allowed a more detailed analysis of M2-Glu channels as described below.

(a) Conductance and current/voltage relationship. Mainly two classes of conductance fluctuations were

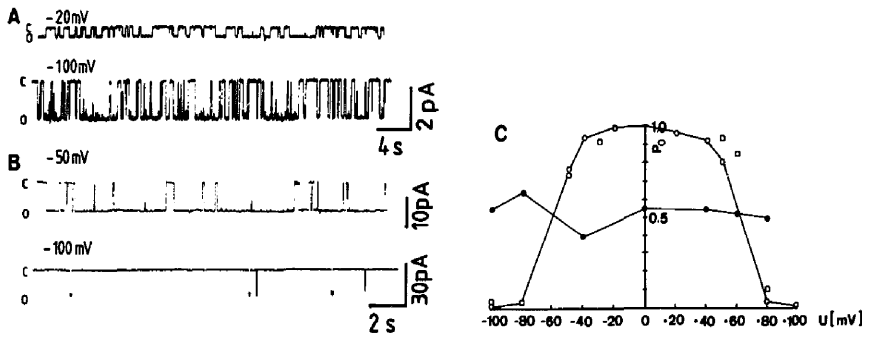

Fig. 6. Voltage dependence of the open probability of M2-Glu induced current fluctuations. (A) Stationary fluctuations of the small M2-Glu induced conductance (approx. 15 pS). (B) Stationary fluctuations of the large conductance (approx. 200 pS). (C) Open probabilities (P_o) of small (filled circles; from one experiment) and large (open circles, squares; two experiments) M2-Glu fluctuations plotted against transbilayer voltage.

observed: one with a conductance of 25 ± 5 pS (mean ± S.D., $n = 3$ bilayers) and one of about 100 to 300 pS in 0.1 M KCl (Fig. 6A, B). Both types of conductivities exhibited linear I/V relationships between + and − 100 mV in the absence of an ion gradient (not shown but see Fig. 5).

(b) M2-Glu channels are cation-selective. The M2-Glu induced conductances were cation-selective in all experiments. When reversal potentials were determined for bilayers containing several channels, the calculated permeability ratios peaked at $P_K/P_{Cl} \approx 5$ (4 bilayers, 27 determinations; Fig. 4A). Cation selectivity was also observed on the single channel level for both types of fluctuations induced by M2-Glu. For large fluctuations, values of P_K/P_{Cl} from 3.5 to 16 (average 6 ± 3, mean ± S.D., $n = 4$ bilayers) were determined by recording current/voltage relationships in the presence of KCl concentration gradients. Fig. 5 shows one of these curves which is characterized by $P_K/P_{Cl} = 12$. For small current fluctuations, P_K/P_{Cl} values of 8 and 26 were obtained ($n = 2$ bilayers). We infer these pronounced cation selectivities to be related to the negative terminal charges of peptide M2-Glu.

(c) Voltage dependence of the open probability. The small and large conductance fluctuations showed remarkable differences with respect to the voltage dependence of the probability to be in the open state (P_o). The open probability of small fluctuations was approx. 0.5 and nearly voltage independent between + and − 100 mV (Fig. 6A, C). P_o of large fluctuations was close to 1.0 at 0 mV and decreased strongly when approaching + and − 100 mV (Fig. 6B, C). This suggests that large and small M2-Glu channels represent structurally different channel populations.

(d) Gating mechanism. Fig. 7 shows that the large M2-Glu induced conductances may fluctuate between the closed (C) and several open (O) states. Direct transitions between the different states (e.g., C ↔ O2, C ↔ O3, O2 ↔ O3, O3 ↔ O1) suggest them to represent substates of one and the same channel complex rather than independent channel entities. Further, there is evidence that the channels formed are capable of repeated open-closed cycles without disintegration. During long observation periods (≫ 10 min), no multiples of the main conductance states were seen although the channels performed many open-closed transitions ($n \gg 100$) at P_o close to 1.0. Also, periods of channel activity were often separated by silent periods ($P_o = 0$) lasting for several minutes. For statistical reasons, such behavior is not expected if each opening and closing event corresponds to the assembly and disintegration of a channel complex from a large pool of monomers. Silent channels could be reactivated by changing voltage. Fig. 8 shows typical experiments where after silent periods at −80 mV voltage was briefly removed. Immediately after returning to −80 mV, channel openings could be observed.

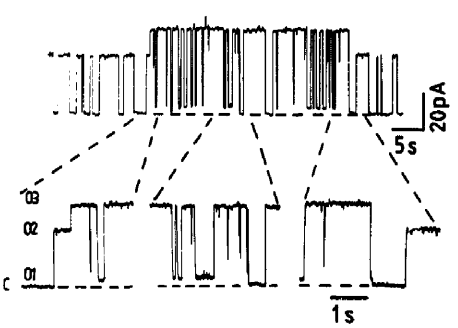

Fig. 7. Complex gating behavior of the M2-Glu induced conductance. Current fluctuations include a closed (C) and three open states (O1 to O3) (recorded at +50 mV). The lower trace shows direct transitions between states C and O2, O2 and O1, O2 and O3, and O3 and C, respectively, on an extended time scale.

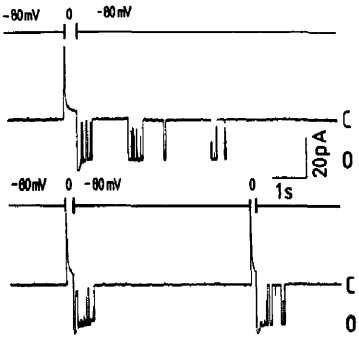

Fig. 8. Rapid reappearance of current fluctuations after brief removal of transbilayer voltage. The upper trace shows the immediate occurrence of current fluctuations at −80 mV after a brief (0.4 s) removal of voltage (○). No current fluctuations had occurred during 100 s before voltage removal. The lower trace shows the effect of two successive transitions between −80 mV and 0 mV.

For the hydrophobic peptide M4, stably increased conductivities of different magnitude (Fig. 3) were observed which were characterized by near linear I/V relationships (not shown). This peptide also induced erratic increases in conductivity which are similar to the effects of bilayer perturbation caused by surface active agents [26]. No repetitive opening and closing of discrete channels occurred, however, with this peptide (16 experiments) although very fast fluctuations (in the millisecond range) may have escaped detection. We interpret the stably increased conductivities to result from ion conducting structures made of peptide M4.

Discussion

In this study we show that synthetic peptides derived from the predicted transmembrane domains M2 and M4 of the GlyR α subunit are capable of increasing the ion permeability of lipid vesicle membranes. The conductance induced by peptides M2 and M2-Glu were shown to result from rectangular channel-like conductance fluctuations. The conductances induced by peptide M4, in contrast, did not exhibit such repetitive fluctuations.

In light of models proposed for the homologous nAChR [27–29], the pore intrinsic to the GlyR may be formed by α-helical M2 segments contributed from five subunits [11]. Segment M4, on the other hand, is thought to be located at the protein/lipid interface of the GlyR's membrane spanning portion [30].

Notably and consistent with its hypothesized role in ion conduction, only channels made of the M2 type of peptides displayed repetitive gating. The large diversity of conductances observed, however, contrasts the four defined substates (12–46 pS) found for the GlyR by patch clamp analysis [15]. This heterogeneity of channel events is consistent with a model where different levels of single-channel conductance are attributed to a variable number of peptide monomers in the oligomeric channels, i.e., different channel cross-sections. It might be argued that the increased thickness of decane-solvated bilayers with respect to natural membranes accounts for the discrepancy between M2 peptide channels and native GlyR. Increasing bilayer thickness would be expected to destabilize an oligomeric peptide channel complex, i.e., decrease its life-time and conductance. Therefore, the greatly increased values of these properties of our M2 peptide channels versus native GlyR [15] as observed here are unlikely to result from the larger thickness of our bilayers.

The exquisite anion selectivity of the GlyR [15] was not mimicked by any of our peptides. Rather, M2 channels formed anion-selective as well as cation-selective channels. Conceivably, structurally different M2 channel populations account for this diversity. Generally, it is thought that the cation selectivity of uncharged peptide ion channels and ion carriers is due to the negative potentials of carbonyl oxygens of the peptide backbone [31]. On the other hand, the positive terminal charges of the M2 peptide are expected to favour anion selection by the M2 channels. As a net result, the ion selectivity of M2 channels may vary with the distance of the charges from the channel mouth. Interestingly, conversion of the terminal charges of M2 modulated ion selectivity in the expected fashion. Introduction of two negative head groups resulted in the exclusive formation of cation selective M2-Glu channels.

This effect of terminal charges on ion selection is consistent with the view [5] that the positive charges bordering the M2 segment of the GlyR α subunit account for the receptor's anion binding sites determined electrophysiologically [15].

An interesting feature of the M2-Glu channel is its kinetic stability as evidenced by its considerable life-time. In this respect, the M2-Glu channel behaves like a stable proteinaceous pore rather than gramicidin channels which close by disintegration of the channel complex [32]. For constituting a channel of defined size and ion-selectivity, however, the geometric constraints imposed by fixation of transmembrane domains within large proteins seem essential.

The finding that not only the hydroxylated M2 type of peptides but also the hydrophobic peptide M4 increased membrane conductivity, suggests that a high content of hydrophilic amino acids in the peptides is not required for allowing ion passage. This interpretation is consistent with the ability of other largely hydrophobic synthetic peptides [33,34] or naturally occurring peptide ionophores [35] to form channels in the black lipid bilayer system. Moreover, it implies that conductivity induced by individual hydrophobic peptides is not

a valid criterion to qualify the latter as pore lining segments in proteinaceous channels.

Concluding remarks

Previously, peptides corresponding to the putative pore lining segments Sc_1 of the voltage-dependent Na channel [17] and M2 of the nAChR [18] were shown to form cation-selective channels in lipid bilayers. The reported single-channel conductances and life-times of these peptide channels included values characteristic of the native channel proteins but were scattered over a large range. Nevertheless, the approach was suggested to be a valuable tool for studying the pore-lining parts of channel proteins. Here, we found an even larger discrepancy between GlyR M2 peptide channels and native GlyR with respect to ion-selectivity, conductance and life-time. We therefore conclude that results obtained by reconstitution of synthetic transmembrane domains are only of limited significance at least for the investigation of anion channel proteins.

Acknowledgements

We gratefully acknowledge E. Harbich for help with the bilayer experiments, E. Lewitzki for recording the CD-spectra, C. Grund and Dr. W. Franke for electron microscopy, Dr. R. Pipkorn and E. Bernath for peptide synthesis. We thank our colleagues L. Thomas, V. Schmieden and Dr. O. Taleb for critically reading the manuscript, and I. Veit-Schirmer for its preparation. This work was supported by the Bundesministerium für Forschung und Technologie, Deutsche Forschungsgemeinschaft (SFB 317) and the Fonds der Chemischen Industrie. D.L. was a predoctoral fellow of the Fonds der Chemischen Industrie.

References

1 Catterall, W.A. (1988) Science 242, 50–61.
2 Noda, M., Takahashi, H., Tanabe, T., Toyosato, M., Kikyotani, S., Furutani, Y., Hirose, T., Takashima, H., Inayama, S., Miyata, T. and Numa, S. (1983) Nature 302, 528–532.
3 Boulter, J., Evans, K., Goldman, D., Martin, G., Treco, D., Heinemann, S. and Patrick, J. (1986) Nature 319, 368–374.
4 Hermans-Borgmeyer, I., Zopf, D., Ryseck, R.-P., Hovemann, B., Betz, H. and Gundelfinger, E.D. (1986) EMBO J. 5, 1503–1508.
5 Grenningloh, G., Rienitz, A., Schmitt, B., Methfessel, C., Zensen, M., Beyreuther, K., Gundelfinger, E.D. and Betz, H. (1987) Nature 328, 215–220.
6 Schofield, P.R., Darlison, M.G., Fujita, N., Burt, D.R., Stephenson, F.A., Rodriguez, H., Rhee, L.M., Ramachandran, J., Reale, V., Glencorse, T.A., Seeburg, P.H. and Barnard, E.A. (1987) Nature, 328, 221–227.
7 Hucho, F.L., Oberthür, W. and Lottspeich, F. (1986) FEBS Lett. 205, 137–142.
8 Giraudat, J., Dennis, M., Heidmann, T., Haumont, P.T., Lederer, F. and Changeux, J.P. (1987) Biochemistry 26, 2410–2418.
9 Imoto, K., Methfessel, C., Sakmann, B., Mishina, M., Mori, Y., Konno, T., Fukuda, K., Kurasaki, M., Bujo, H., Fujita, Y. and Numa, S. (1986) Nature 324, 670–674.
10 Betz, H. and Becker, C.-M. (1988) Neurochem. Int. 13, 137–146.
11 Langosch, D., Thomas, L. and Betz, H. (1988) Proc. Natl. Acad. Sci. USA 85, 7394–7398
12 Graham, D., Pfeiffer, F. and Betz, H. (1983) Eur. J. Biochem. 131, 519–525.
13 Schmieden, V., Grenningloh, G., Schofield, P.R. and Betz, H. (1989) EMBO J. 8, 695–700.
14 Sontheimer, H., Becker, C.-M., Pritchett, D.B., Schofield, P.R., Grenningloh, G., Kettenmann, H., Betz, H. and Seeburg, P.H. (1989) Neuron 2, 1491–1497.
15 Bormann, J., Hamill, O.P. and Sakmann, B. (1987) J. Physiol. 385, 243–286.
16 Hamill, O.P., Bormann, J. and Sakmann, B. (1983) Nature 305, 805–808.
17 Oiki, S., Danho, W. and Montal, M. (1988) Proc. Natl. Acad. Sci. USA 85, 2393–2397.
18 Oiki, S., Danho, W., Madison, V. and Montal, M. (1988) Proc. Natl. Acad. Sci. USA 85, 8703–8707.
19 Merrifield, R.B. (1963) J. Am. Chem. Soc. 85, 2149–2154.
20 Adler, A.J., Greenfield, N.J. and Fasman, G.D. (1973) Methods Enzymol. 27, 675–735.
21 Sims, P.J., Waggoner, A.S., Wang, C.-H., and Hoffman, J.F. (1974) Biochemistry 13, 3315–3330.
22 Mueller, P., Rudin, D.O., Tien, H.T. and Wescott, W.C. (1963) J. Phys. Chem. 67, 534–535.
23 Cohen, S.C., Myles, H.A., Zimmerberg, J. and Finkelstein, A. (1984) J. Cell Biol. 98, 1054–1062.
24 Greenfield, N. and Fasman, G.D. (1969) Biochemistry 8, 4108.
25 Hodgkin, A.L. and Katz, B. (1949) J. Physiol. 108, 37–77.
26 Gögelein, H. and Hübi, A. (1984) Biochim. Biophys. Acta 773, 32–38.
27 Changeux, J.P., Giraudat, J. and Dennis, M. (1987) Trends Pharmacol. Sci. 8, 459–465.
28 Unwin, N. (1989) Neuron 3, 665–676.
29 Betz, H. (1990) Biochemistry 29, 3591–3599.
30 Langosch, D., Betz, H. and Becker, C.-M. (1990) in Glycine Neurotransmission (Ottersen, O. and Strom-Mathisen, J., eds.), Wiley, New York.
31 Eisenmann, G. and Dani, J.A. (1987) Annu. Rev. Biophys. Biophys. Chem. 16, 205–226.
32 Bamberg, E. and Läuger, P. (1973) J. Membr. Biol. 11, 177–194.
33 Molle, G., Dugast, J.Y., Duclohier, H., Daumas, P., Heitz, F. and Spach, G. (1988) Biophys. J. 53, 193–203.
34 Menestrina, G., Voges, K.-P., Jung, G. and Boheim, G. (1986) J. Membr. Biol. 93, 111–132.
35 Latorre, R. and Alvarez, O. (1981) Physiol. Rev. 61, 77–151.